The Silver Lining of a Viral Agent: Increasing Seed Yield and Harvest Index in Arabidopsis by Ectopic Expression of the Potato Leaf Roll Virus Movement Protein[1]

Kristin Kronberg, Florian Vogel, Twan Rutten, Mohammed-Reza Hajirezaei, Uwe Sonnewald, and Daniel Hofius*

Institut für Pflanzengenetik und Kulturpflanzenforschung, D–06466 Gatersleben, Germany (K.K., T.R., M.-R.H.); Friedrich-Alexander-Universität Erlangen-Nürnberg, Lehrstuhl für Biochemie, 91058 Erlangen, Germany (F.V., U.S.); and Department of Molecular Biology, Copenhagen Biocenter, University of Copenhagen, 2200 Copenhagen N, Denmark (D.H.)

Ectopic expression of viral movement proteins (MPs) has previously been shown to alter plasmodesmata (PD) function and carbon partitioning in transgenic plants, giving rise to the view of PD being dynamic and highly regulated structures that allow resource allocation to be adapted to environmental and developmental needs. However, most work has been restricted to solanaceous species and the potential use of MP expression to improve biomass and yield parameters has not been addressed in detail. Here we demonstrate that MP-mediated modification of PD function can substantially alter assimilate allocation, biomass production, and reproductive growth in Arabidopsis (*Arabidopsis thaliana*). These effects were achieved by constitutive expression of the potato leaf roll virus 17-kD MP (MP17) fused to green fluorescent protein (GFP) in different Arabidopsis ecotypes. The resulting transgenic plants were analyzed for PD localization of the MP17:GFP fusion protein and different lines with low to high expression levels were selected for further analysis. Low-level accumulation of MP17 resulted in enhanced sucrose efflux from source leaves and a considerably increased vegetative biomass production. In contrast, high MP17 levels impaired sucrose export, resulting in source leaf-specific carbohydrate accumulation and a strongly reduced vegetative growth. Surprisingly, later during development the MP17-mediated inhibition of resource allocation was reversed, and final seed yield increased in average up to 30% in different transgenic lines as compared to wild-type plants. This resulted in a strongly improved harvest index. The release of the assimilate export block was paralleled by a reduced PD binding of MP17 in senescing leaves, indicating major structural changes of PD during leaf senescence.

Plant cells are interconnected by unique membrane-lined channels in the cell wall, termed plasmodesmata (PD), that provide cytoplasmic continuity for cell-to-cell transport and communication. PD form the symplastic network for photosynthate supply into the minor vein tissue of mature source leaves, and also contribute substantially to the unloading of assimilates into developing sink organs (Stitt, 1996; Imlau et al., 1999; Baluska et al., 2001; Haupt et al., 2001; Viola et al., 2001; Hoth et al., 2005). Although formerly seen as simple pores with a low molecular size exclusion limit (SEL) that allow only the passage of small metabolites, PD have now been shown to be dynamic structures that also facilitate the specific trafficking of large RNA and protein macromolecules involved in local and systemic signaling (Lucas and Lee, 2004; Oparka, 2004; Ruiz-Medrano et al., 2004; Kim and Zambryski, 2005). Beside the observation that apertures of individual PD fluctuate considerably in response to environmental cues, fundamental changes in plasmodesmal architecture and function have been detected during development and in different plant tissues (Crawford and Zambryski, 2001; Roberts and Oparka, 2003; Zambryski, 2004; Liarzi and Epel, 2005). Most remarkably, plasmodesmal permeability is considerably down-regulated during the sink-source transition in leaves, which is accompanied by a progressive conversion from simple to branched forms of PD (Oparka et al., 1999; Roberts et al., 2001). This close correlation between the importing-exporting transition for photoassimilates and changes in plasmodesmal conductivity suggested that PD may act as important control sites for symplastic assimilate transport and resource allocation between source and sink tissues (Lucas and Wolf, 1999; Lucas and Lee, 2004).

Compelling evidence for this hypothesis has been provided by studies on virus-encoded movement proteins (MPs), which are well known to localize to secondary branched PD, to substantially increase the basal plasmodesmal SEL, and to facilitate cell-to-cell transfer of MP-bound viral genomes through PD (Wolf et al., 1989, 1991; Ding et al., 1992; Waigmann et al., 1994; Itaya et al., 1998; Lazarowitz and Beachy, 1999; Oparka et al., 1999; Hofius et al., 2001; Lucas, 2006). Ectopic

[1] This work was supported by a grant from the Deutsche Forschungsgemeinschaft (grant no. DFG SO 300/9/1).

* Corresponding author; e-mail hofius@my.molbio.ku.dk.

The author responsible for distribution of materials integral to the findings presented in this article in accordance with the policy described in the Instructions for Authors (www.plantphysiol.org) is: Uwe Sonnewald (usonne@biologie.uni-erlangen.de).

www.plantphysiol.org/cgi/doi/10.1104/pp.107.102806

expression of MPs from *Tobacco mosaic virus* (TMV) and *Cucumber mosaic virus* (CMV) in transgenic tobacco (*Nicotiana tabacum*), potato (*Solanum tuberosum*), and melon (*Cucumis melo*) plants resulted in dilated PD accompanied by remarkable changes of carbohydrate metabolism and biomass partitioning (Lucas et al., 1993; Balachandran et al., 1995; Lucas et al., 1996; Shalitin et al., 2002). These MP-exerted alterations, however, differed strongly with respect to plant species, tissue specificity of the promoters, as well as developmental stages. For instance, expression of the TMV-MP in transgenic tobacco plants under control of a constitutive promoter (Balachandran et al., 1995; Olesinski et al., 1995) as well as expression under a phloem-restricted promoter in transgenic potato plants (Almon et al., 1997) resulted in carbohydrate accumulation and decreased Suc export from source leaves. In contrast, expression of TMV-MP from the green tissue-specific ST-LS1 promoter in potato as well as from a virus vector in melon plants caused lower carbohydrate contents and higher Suc export rates (Olesinski et al., 1996; Shalitin et al., 2002). These findings gave rise to a model, in that MPs interfere with the plasmodesmal trafficking of macromolecular signals involved in carbohydrate metabolism and source-sink regulation (Lucas et al., 1996; Lucas and Wolf, 1999). However, recent analysis of tomato spotted wilt virus (TSWV) MP (NS_M) expressing tobacco plants showed that the severe infection-like and Suc export-deficient phenotype was correlated with heat-reversible obstruction of NS_M-targeted mesophyll PD by callose or 1,3-β-D-glucan deposition (Rinne et al., 2005). Based on these results, the authors postulated that the impact of MP on source leaf functioning is the consequence of a basal defense response to prolonged MP accumulation at PD rather than a direct influence on carbohydrate metabolism and transport.

In addition to the MPs of TMV, CMV, and TSWV, the 17-kD MP (MP17) of the phloem-limited potato leaf roll polerovirus (PLRV) has been used as another model system to study the consequences of altered PD function for symplastic assimilate transport and sink-source relations (Herbers et al., 1997; Hofius et al., 2001). Initially, a strong impact of PLRV-MP17 on carbon metabolism and biomass allocation was demonstrated by constitutive expression of an aminoterminally extended MP17 version (MP17N) in transgenic tobacco plants (Herbers et al., 1997). Several MP17N transgenic lines showed severe growth retardation and bleached intercostal regions on source leaves paralleled by a drastic accumulation of carbohydrates, altered gene expression, and a limited cross protection toward potato virus Y infection. In addition, cell biological studies using MP17N and nonphenotypic MP17:GFP expressing transgenic lines demonstrated an overall affinity of MP17 to branched PD in vascular and nonvascular tissue of source leaves as well as an increase of plasmodesmal SEL in mesophyll cells (Herbers et al., 1997; Hofius et al., 2001). Interestingly, plasmodesmal targeting and gating capacity of MP17 appeared to be independent of MP17 protein amount, whereas carbohydrate status and viral resistance followed a dosage-dependent mechanism. At low MP17 expression level, transgenic lines showed decreased sugar contents and accelerated spread of potato virus Y infection possibly due to increased PD permeability, while carbohydrate accumulation, growth retardation, and viral defense reactions seemed to be the consequence of rather indirect metabolic effects at high MP17 levels (Hofius et al., 2001).

So far, studies on the mode(s) of action underlying the various MP-induced metabolic and phenotypic responses have mainly concentrated on solanaceous species, and the potential use of MP to manipulate resource allocation for the benefit of leaf biomass and seed production has not been addressed in detail. The aim of this study, therefore, was to establish how constitutive expression of PLRV-MP17 affects PD functioning in terms of carbon partitioning, resource allocation, and productivity in the Arabidopsis (*Arabidopsis thaliana*) plant model. We demonstrate that GFP-tagged MP17 localized to branched PD in various cell types, and caused alteration of carbohydrate status, biomass accumulation, and seed yield in an ecotype-independent but strict dosage-dependent manner. Low expression of MP17 resulted in increased vegetative biomass production, whereas high protein levels impaired assimilate export as evident by starch accumulation in source leaves and severe growth retardation. At later stages of plant development, however, the inhibition of assimilate export was released, resulting in improved seed yield and a considerably enhanced harvest index probably due to mobilization and allocation of excess carbohydrate pools. Importantly, the reversion of the symplastic transport block was paralleled by a reduced accumulation of MP17 protein at PD, suggesting changes of plasmodesmatal architecture and function during the progression of leaf senescence.

RESULTS

Association of MP17 with PD in Arabidopsis

To generate PLRV-MP17 expressing Arabidopsis plants, a binary construct harboring a *MP17:GFP* gene fusion under control of the constitutive cauliflower mosaic virus (CaMV) 35S promoter (p35S-1; Hofius et al., 2001) was used for *Agrobacterium*-mediated transformation of Columbia-0 (Col-0) and C24 ecotypes. Primary T1 transformants were screened by western-blot analysis using a MP17-specific antibody (Hofius et al., 2001; data not shown). Independent Col-0 and C24 lines accumulating considerable amounts of the MP17:GFP fusion protein were selected and subsequently analyzed for subcellular localization of the MP17:GFP fusion protein by fluorescence and electron microscopy. Punctate GFP-derived fluorescence signals could be detected in association with cell walls in the epidermis (Fig. 1C), mesophyll (Fig. 1D), and vasculature (Fig. 1E) of source leaves as well as in the vascular bundles of the root

central cylinder (Fig. 1F). In contrast, MP17:GFP accumulation in sink leaves was detectable only at trichomes (Fig. 1B) and was absent from immature cell types, including the epidermal layer (Fig. 1A). Immunogold labeling with anti-MP17 antiserum verified that the observed GFP fluorescence pattern was due to specific MP17:GFP accumulation at PD of mature nonvascular and vascular cell types (Fig. 1, G and H), indicating a similar affinity of MP17 to branched PD as seen before in MP17N and MP17:GFP transgenic tobacco plants (Hofius et al., 2001). Antibody specificity was confirmed by incubating wild-type Arabidopsis leaf sections with anti-MP17 antibodies, which did not result in any immunogold labeling of PD in mesophyll and vascular tissue (Fig. 1, I and J).

MP17 Expression Alters Carbohydrate Levels, Biomass Accumulation, and Reproductive Growth in Different Arabidopsis Ecotypes

MP17-mediated alterations of carbohydrate status, biomass allocation, and phenotypic appearance were previously shown to be strictly dependent on MP17 protein amounts in transgenic tobacco plants (Hofius et al., 2001). Hence, three homozygous lines with variable levels of MP17:GFP fusion protein were selected for both Arabidopsis ecotypes, respectively, and subjected to quantitative western-blot analysis using the polyclonal MP17 antibody (Fig. 2, D and E). In the Col-0 background, line Col-16 showed the highest accumulation of MP17:GFP protein (hereafter referred to as 100%) whereas lines Col-14 and Col-9 accumulated MP17:GFP to a medium (78%) and low level (28%) in relation to Col-16, respectively. MP17:GFP protein in selected C24 lines reached 80% (line C24-74), 45% (C24-84), and 30% (C24-81) of the level in Col-16, respectively.

Phenotype and growth analysis of transgenic lines at short-day (SD) conditions (6 weeks) revealed remarkable changes in biomass allocation in response to different MP17:GFP amounts (Fig. 2, A and B). Low-level accumulation of the fusion protein in lines Col-9 and C24-81 resulted in increased aboveground biomass production of 16% and 41% compared to the controls, respectively, but failed to reach statistical significance for C24-81. In contrast, high-level MP17 expression in Col-16 and C24-74 caused considerable growth retardation as evident by reduced biomass accumulation to only 13% (Col-16) and 30% (C24-74) of the respective wild-type plants (Fig. 2, G and H). To further analyze whether the MP17-induced growth penalty was due to impaired assimilate export as previously demonstrated for MP17 expressing tobacco plants (Hofius et al., 2001), steady-state levels of carbohydrates were determined in a plant set grown under SD conditions in parallel to the lines used for vegetative biomass analysis. As shown in Table I, highest MP17 expression and lowest biomass accumulation in line Col-16 was accompanied by strong accumulation of soluble sugars and starch in source leaves, suggesting a MP17-mediated blockage of photosynthate export. Less severe growth inhibition in C24-74 was associated with only a minor increase in overall carbohydrate levels, whereas increased biomass production in low-level expressing lines Col-9 and C24-81 seemed to be paralleled by a slight reduction of both Suc and starch contents. These data suggested a dosage-dependent impact of MP17 expression on assimilate allocation from source leaves, which seem to have either beneficial or detrimental consequences for vegetative biomass accumulation at low and high expression levels, respectively.

To further elucidate whether MP17-induced changes of photosynthate export also influence the transition from vegetative to reproductive growth as well as the reproductive outcome, i.e. seed production, transgenic lines were shifted after 6 weeks from SD to long-day (LD) conditions. Determination of assimilate accumulation in leaves of the various lines grown under these flowering inducing conditions revealed similar results as demonstrated for the SD-grown plants (data not shown). Interestingly, flowering initiation in low and modestly expressing lines C24-81, C24-84, and Col-9 was significantly accelerated by approximately 6, 3, and 1 d compared to wild type, respectively (Fig. 2, J and K). In contrast, high-level accumulation of MP17 in lines Col-16 and C24-74 resulted in delayed flowering by 6 and 7 d relative to the controls, suggesting that the dosage-dependent impact of MP17 on carbohydrate partitioning and vegetative biomass accumulation was correlated with specific alterations of reproductive development. Consequently, seed yield was determined for the various lines after all plants were completely senescent and siliques on the main inflorescence started to open. Surprisingly, highest MP17 expression in the severely growth-retarded line Col-16 caused a consistent increase in seed yield by 12.6%, 37.8%, and 42.8% (in average 29.9%, $P < 0.001$) in three independent growth sets compared to the wild-type control, respectively, whereas seed production appeared to be largely unaltered in the lower expressing transgenic lines Col-9 and Col-14 (Fig. 2M). Reproductive outcome of C24 lines was either unaffected or even slightly reduced in line C24-81, which showed the highest leaf biomass accumulation under SD conditions (Fig. 2N). These results indicated an upper threshold level for the beneficial impact of transgenic MP17 protein accumulation on seed production and additionally suggested a close interrelationship between MP17-induced carbohydrate accumulation, growth penalty, and improved yield.

To investigate whether enhanced seed production in Col-16 was solely the consequence of high MP17 expression level or rather due to ecotype-specific effects, we introduced the 35S-MP17:GFP construct into the Landsberg *erecta* (L*er*) ecotype and screened for transgenic lines that showed a severe growth inhibition and comparably high MP17 amounts as Col-16. Two lines, termed L*er*-1 and L*er*-12, were identified that exhibited strong MP17:GFP-derived fluorescence at PD (data not shown) and exceeded the transgene protein level in

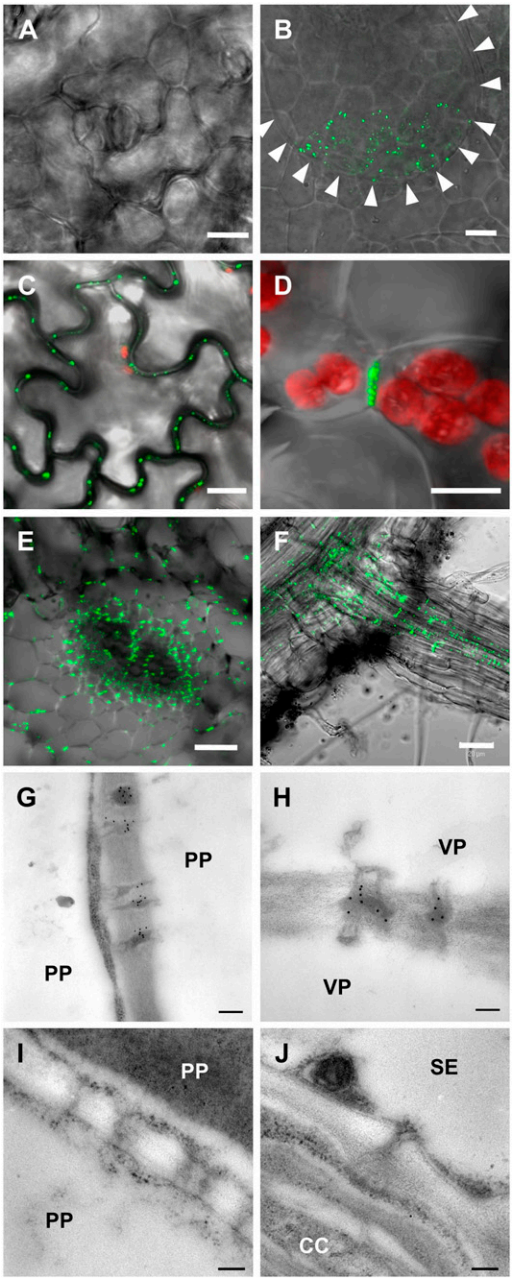

Figure 1. Association of MP17:GFP with PD in various cell types of transgenic Arabidopsis plants (line Col-16). A and B, Epidermal cells of sink leaves. GFP-derived signals are not detectable in the cell walls of adjacent cells (A) but decorate the contact zone of trichome base cell-epidermal cell connection (B). Arrowheads in B mark the borders and orientation of the trichome base cell. C, Epidermis of mature source leaves showing green fluorescent dots at all cell-to-cell junctions. D, Longitudinal section through the spongy parenchyma tissue in the mesophyll of a mature source leaf showing GFP fluorescence at the connecting wall of two parenchyma cells. Red fluorescence originates from chlorophyll in the chloroplasts. E, Cross section through the vasculature of a class I vein (midrib) from a mature source leaf showing strong GFP fluorescence in the cell walls between most of vascular cell types, including bundle sheath, vascular parenchyma, and phloem cells. F, Detection of GFP-derived fluorescence in vascular bundles of the central cylinder in primary and PD between palisade parenchyma (PP) cells of a mature source leaf. H, PD between vascular parenchyma cells (VP) of class I veins from a mature source leaf showing MP17-specific gold labeling. I to K, PD between PP cells (I) in the mesophyll and between a companion cell (CC) and a sieve element (SE) in class I veins from wild-type source leaves showing no unspecific MP17 antibody labeling. Bars in A to D represent 10 μm, in E 50 μm, in F 20 μm, and in G to J 15 μm.

Col-16 by 16% and 12%, respectively (Fig. 2F). Consequently, both lines showed dramatically reduced biomass production that reached only 6% and 8% of the wild-type level after 6 weeks under SD conditions, respectively (Fig. 2I). Consistent with the results in line Col-16, the severe growth phenotype in L*er*-1 and L*er*-12 was accompanied by assimilate export deficiency as revealed from source leaf-specific accumulation of soluble sugar and starch (Table I). Additionally, L*er*-1 and L*er*-12 showed a significantly altered transition from vegetative to reproductive growth as flowering initiation was observed approximately 4 and 6 d later than in the wild type under inducing LD conditions, respectively (Fig. 2L). Most remarkably, seed production in both lines was significantly enhanced by 49% ($P < 0.05$) and 26% ($P < 0.05$) relative to the wild-type control, respectively (Fig. 2O). These data suggested an ecotype-independent relationship between high protein expression, reduced leaf biomass accumulation, and higher seed production.

Alteration of Leaf Biomass Accumulation and Seed Yield Is Correlated with Growth Stage-Specific Changes of Suc Export Rates

To directly link this dosage-dependent and inversely related impact of MP17 on biomass and seed production to changes in assimilate allocation, the capacity of source leaves for Suc export was assessed in the different transgenic lines during vegetative and reproductive growth phases. Consistent with improved vegetative biomass accumulation in low-level expressing lines Col-9 and C24-81, Suc efflux rates from detached petioles were slightly (20%), and in case of C24-81, significantly higher than in wild-type plants grown for 6 weeks under SD conditions (Fig. 3, A and C). In contrast, growth-retarded lines L*er*-1, L*er*-12, Col-16, and C24-74 showed considerably reduced Suc concentrations in phloem exudates after the 6-h collection period that reached only 29% to 48% of the respective wild-type controls (Fig. 3, A, C, and E). However, after an additional growth period of 3 weeks under LD conditions, Suc efflux rates in lines Col-16, L*er*-1, and L*er*-12 tended to exceed the respective wild-type level by 15%, 25%, and 31%, respectively (Fig. 3, B and F), which was statistically significant for L*er*-12 ($P < 0.05$). This strongly suggested the reversion of the assimilate export block during the reproductive growth phase.

Collectively, these results indicate that enhanced biomass as well as seed production in low- and high-level

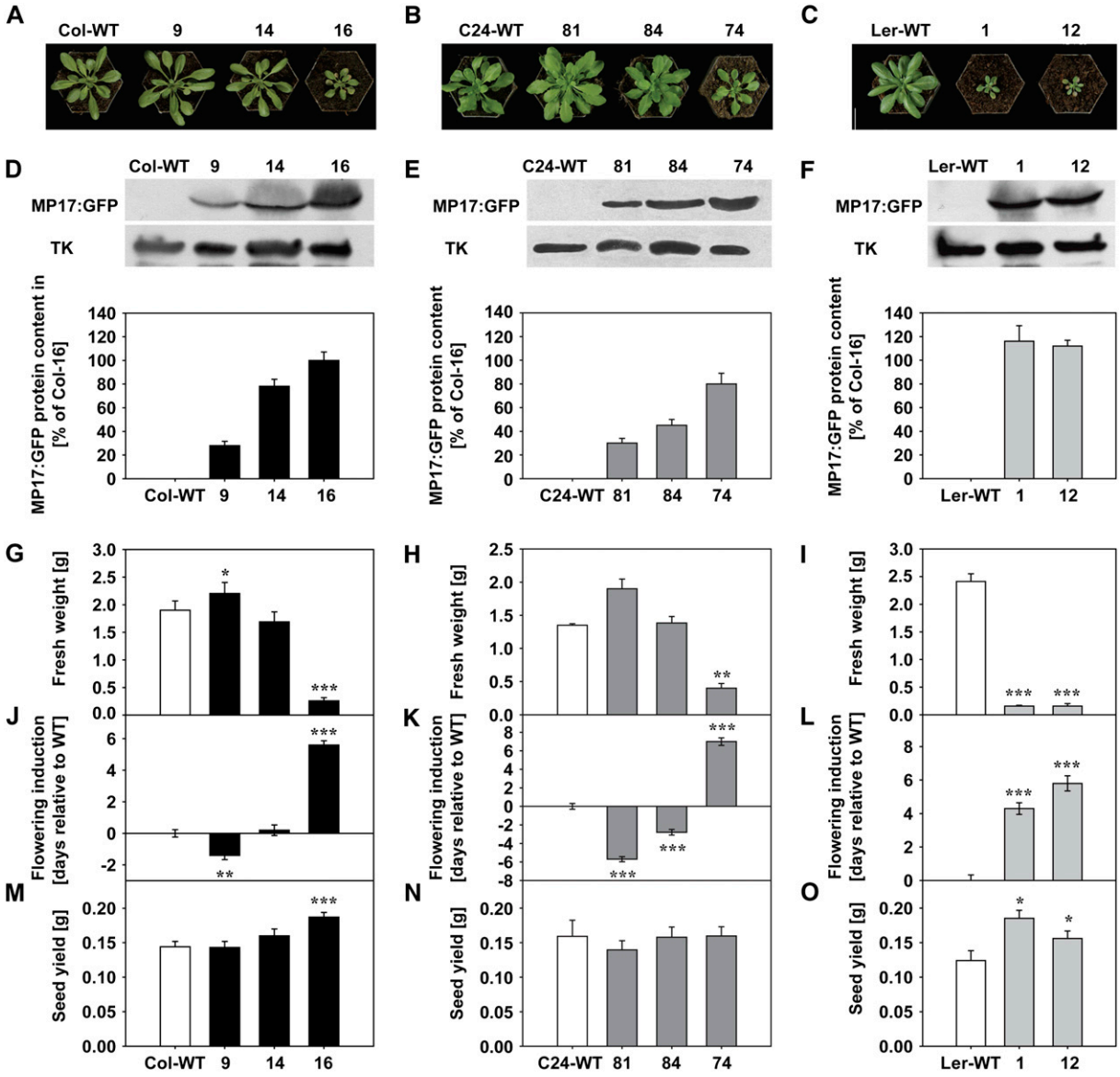

Figure 2. MP17:GFP expression alters vegetative biomass accumulation and reproductive growth in different Arabidopsis ecotypes. A to C, Phenotypic appearance of the indicated MP17:GFP accumulating lines in Col-0 (A), C24 (B), and L*er* (C) background in comparison to the respective ecotype-specific wild-type (WT) control. Plants were grown for 5 weeks under SD conditions. D to F, Immunoblot analysis and quantification of MP17:GFP fusion protein accumulation. Total protein was isolated from mature leaves of the indicated transgenic lines as well as the respective Col-0 (D), C24 (E), and L*er* (F) wild-type controls. Identical amounts of protein were separated by SDS-PAGE, transferred to a nitrocellulose, and probed with a polyclonal anti-MP17 antibody. Immunoblots were developed with an enhanced chemiluminescence detection kit and exposed either to x-ray films (top section) or to an imaging analyzer for real-time detection of the signal strength (bottom figure). Additional incubation of immunoblots with polyclonal anti-Transketolase was taken as control for equal loading and for normalization of the quantified MP17-specific signals. MP17:GFP protein levels were determined in protein extractions of four independent plants per line and values are given as percentage of the protein level in line Col-16. Error bars indicate SD. G to I, Vegetative biomass production in MP17:GFP transgenic lines as compared to the respective wild-type controls. Leaf fresh weight corresponding to the entire plant rosette without the root system was determined after a growth period of 6 weeks under SD conditions. Values for transgenic lines in Col-0 background (G) represent the mean ± SE of three independent experiments, each performed with nine to 12 plants per line. Values for lines in C24 (H) and L*er* (I) ecotypes represent means ± SE of six or at least five individual plants, respectively. J to L, Flowering induction of MP17:GFP transgenic lines. Plants of the indicated lines in the Col-0 (J), C24 (K), and L*er* (L) ecotype together with respective controls were grown for 6 weeks under SD and subsequently shifted to LD conditions. Flowering induction was recorded by counting the days from the date of transfer until the appearance of the first open flower. Values represent means (n = 10) ± SE and are given in days relative to the ecotype-specific wild types. Thus, negative values are indicative of accelerated, positive values of delayed flowering in comparison to the control. M to O, Seed yield of the different MP17:GFP transgenic lines in Col-0 (M), C24 (N), and L*er* (O) ecotypes as compared to the controls. Total seed weight of

expressing lines is associated with growth stage-specific changes in Suc export capacity.

Improved Harvest Index in High-Level MP17:GFP Expressing Arabidopsis Lines

The astonishing finding of an inverse relationship between MP17-mediated alterations in vegetative biomass and yield production implies the potential of substantial changes in harvest index at high expression level. Harvest index is defined as ratio of seed mass and total plant mass and as such serves as indicator of resource allocation toward harvestable organs and important agricultural parameter of plant productivity. To assess changes in harvest index in high-level expressing lines Col-16, L*er*-1, and L*er*-12, plants were grown for 6 weeks at SD before they were shifted to LD conditions to induce reproductive development. Total dry matter production was determined after plants were fully senescent, demonstrating that Col-16, L*er*-1, and L*er*-12 accumulated biomass to approximately 44%, 69%, and 70% of the wild type, respectively (Fig. 4A). This suggested that the induction of reproductive growth partially compensated the dramatic repression of vegetative biomass accumulation in the transgenics under SD conditions and agrees with the observed shift toward enhanced Suc export capacity under prolonged LD conditions. Consistent with the previous results, improved reproductive growth was also manifested by enhanced seed production in all three lines (Fig. 4A), giving rise to a considerably increased harvest index by 2.8-fold in Col-16 ($P < 0.01$) and by 1.8-fold in both L*er*-1 ($P < 0.01$) and L*er*-12 ($P < 0.01$) compared to the ecotype-specific control plants (Fig. 4A).

To explain the higher seed yield upon high-level MP17:GFP expression, we determined the 1,000-seed weight of the three plant lines and found no major changes for all lines compared to the wild-type controls (Fig. 4B), indicating an increase in seed number in the transgenics. Counting the number of siliques per plant revealed a consistent decrease in the transgenic plants relative to the wild types (498 in Col-16 versus 516 in Col-wild type; 302 in L*er*-1 and 298 in L*er*-12 versus 320 in L*er*-wild type, respectively). Thus, the average number of seeds per silique, calculated from 1,000-seed weight, the total seed yield, and the number of siliques is considerably enhanced from approximately 12 in Col-wild type to 15 in Col-16, and from 20 in L*er*-wild type to 25 in both L*er*-1 and L*er*-12 (Fig. 4B).

MP17-Induced Blockage of Assimilate Export Is Released upon Progressing Leaf Senescence

The increased reproductive output in high-level MP17:GFP expressing Col-0 and L*er* lines in association with enhanced Suc export capacity of source leaves during the reproductive growth phases suggests an improved availability and supply of assimilates for generative development. To support this hypothesis, we speculated that the release of MP17-induced export deficiency might also occur as a consequence of progressing leaf age. To test this possibility, fully expanded source leaves (Max) and different leaf stages with progressing senescence from SD-grown Col-16 plants (leaves -6 until -1 with the latter being defined as oldest leaf within the rosette [Fig. 5A]) were assessed for starch accumulation by iodine staining at the end of dark period. As expected, source leaves (Max) of Col-16 exhibited a severe starch excess phenotype compared to the wild-type control. However, starch accumulation seemed to progressively decrease in senescing leaf stages, almost approaching wild-type level in the oldest rosette leaf (-1; Fig. 5B). To further verify these observations, soluble sugars and starch were quantitatively assayed at the indicated leaf stages from 66-d-old Col-16 and wild-type plants at the end of an 8 h light period. A strong decline in starch levels could be confirmed for the different senescing leaf stages compared to maximal amounts reached in the export-deficient source leaf (Max) of Col-16 plants (Fig. 5C). While rosette leaf -6 still exhibited a considerably increased starch level, older leaf stages showed starch accumulation in a comparable range as detected in the presumably export-competent wild-type Max leaf, suggesting a successive reversion of the MP17-mediated export block. Interestingly, in contrast to starch levels, soluble sugars seemed to be increased in older leaf stages (-6 until -4) in relation to Max leaves of line Col-16, and were consistently higher throughout all leaf stages compared to the wild-type level in Max leaves. Importantly, similar changes of starch and soluble sugar levels were also detected upon progressing leaf senescence in Col-16 plants under reproductive, i.e. LD conditions (data not shown). This might indicate an increased turnover of the previously accumulated starch in senescing leaves of Col-16, leading to an enhanced availability of soluble sugars for resource allocation.

Recent evidence suggests that maltose serves as a major metabolic intermediate in conversion of starch to Suc during the night (Chia et al., 2004; Niittyla et al., 2004; Lu and Sharkey, 2006). Hence, elevated levels of maltose are regarded as valuable indicators of impaired

Figure 2. (*Continued.*)
individual plants was determined after a growth period of 42 d under SD and of additional 40 to 50 d under LD conditions. Similar to vegetative biomass production in G, values for lines in Col-0 background represent the mean ± SE of three independent experiments with nine to 12 plants per line, respectively. Data for controls and transgenic lines in C24 and L*er* background are given as mean ± SE of at least eight (C24) or nine (L*er*) individual plants. Asterisks indicate statistical differences between transgenic lines and the respective wild type at *, $P < 0.05$; **, $P < 0.01$; and ***, $P < 0.001$ as determined by the Mann-Whitney *U*-test.

Table I. *Carbohydrate levels in leaves of three different MP17:GFP transgenic Arabidopsis ecotypes*

Leaf samples were harvested 7 h after beginning of the light period. Plants were grown for 5 weeks under SD conditions and samples were collected from fully expanded source leaves. Two samples were taken from each plant and averaged; values represent the mean ± SE of 10 (Col-0 and L*er* lines) or at least five (C24 lines) independent plants. Asterisks indicate statistical differences between transgenic lines and the respective wild type at *, $P < 0.05$; **, $P < 0.01$; and ***, $P < 0.001$ as determined by the Mann-Whitney *U*-test.

Plant Line	Glc	Fru	Suc	Starch	Sol Sugars/Starch
	mmol m^{-2}	*mmol m*$^{-2}$	*mmol m*$^{-2}$	*mmol m*$^{-2}$	
Col-wild type	0.48 ± 0.06	0.92 ± 0.11	1.15 ± 0.07	11.29 ± 0.46	0.23 ± 0.01
Col-9	0.52 ± 0.06	1.87 ± 0.36	0.99 ± 0.08	10.43 ± 0.56	0.32 ± 0.03*
Col-14	1.01 ± 0.15**	1.64 ± 0.06***	1.07 ± 0.07	10.88 ± 0.43	0.34 ± 0.01***
Col-16	5.26 ± 0.54***	2.11 ± 0.16***	2.65 ± 0.24***	23.10 ± 2.01***	0.44 ± 0.02***
C24-wild type	1.18 ± 0.15	1.02 ± 0.18	1.00 ± 0.06	13.05 ± 0.66	0.25 ± 0.03
C24-81	0.92 ± 0.12	0.93 ± 0.12	0.78 ± 0.06**	12.05 ± 0.85	0.22 ± 0.01
C24-84	0.84 ± 0.07	1.08 ± 0.09	0.79 ± 0.06*	13.90 ± 0.93	0.20 ± 0.01
C24-74	1.10 ± 0.15	1.20 ± 0.10	1.09 ± 0.06	14.76 ± 0.52	0.20 ± 0.01
L*er*-wild type	0.82 ± 0.10	1.62 ± 0.13	1.21 ± 0.04	12.04 ± 0.43	0.30 ± 0.02
L*er*-1	5.52 ± 0.58***	4.72 ± 0.37***	2.48 ± 0.15***	17.10 ± 1.26**	0.78 ± 0.09***
L*er*-12	3.49 ± 0.61***	3.37 ± 0.29***	2.02 ± 0.26**	13.21 ± 1.43	0.76 ± 0.16***

starch mobilization and disturbed assimilate export capacity in source leaves. Consequently, maltose levels were determined in the different leaf stages of Col-16 and wild type at the end of the 16-h dark period. In agreement with the observed starch excess phenotype and proposed assimilate export block, Max source leaves of Col-16 showed 2.4-fold higher maltose concentrations than the comparable leaf stage of the wild-type control (Fig. 5C). In contrast, rosette leaf stages -6 until -1 showed decreased levels of maltose that were consistently lower than the level in the wild-type Max leaf. This decrease could not be explained by lowered starch levels, since leaf stage -6 accumulated considerably more starch than the wild-type max leaf. Thus, it rather suggests the release of the MP17-induced export block resulting in successive mobilization of starch reserves upon leaf senescence.

Reduced MP17:GFP Accumulation at PD Causes Reversion of Symplastic Transport Block upon Leaf Senescence

The strict dosage-dependent impact of PD-localized MP17 on carbon levels and export capacity in source

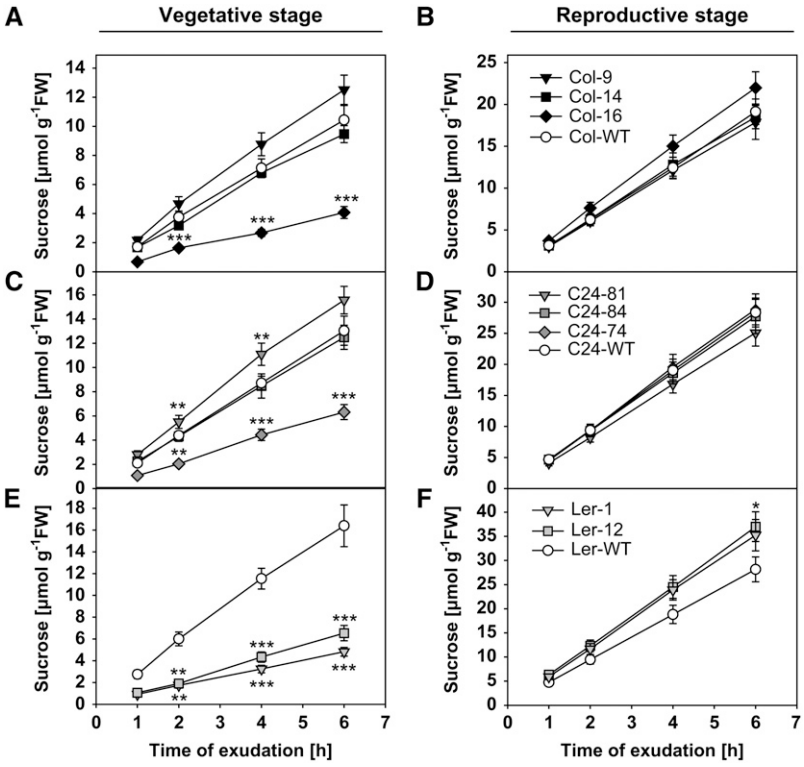

Figure 3. Suc efflux from source leaves of various MP17:GFP transgenic lines during vegetative and reproductive growth. Phloem exudates were collected from two mature source leaves per line after a growth period of 6 weeks under SD conditions (vegetative stage) and after additional 3 weeks under LD conditions (reproductive stage). Suc content in the exudates was determined 1, 2, 4, and 6 h after excision for the indicated lines in the Col-0 (A and B), C24 (C and D), and L*er* (E and F) background in comparison to the respective controls. Data are presented as means ± SE of five individual plants per line. Asterisks indicate statistical differences between transgenic lines and the respective wild type at *, $P < 0.05$; **, $P < 0.01$; and ***, $P < 0.001$ as determined by the Mann-Whitney *U*-test.

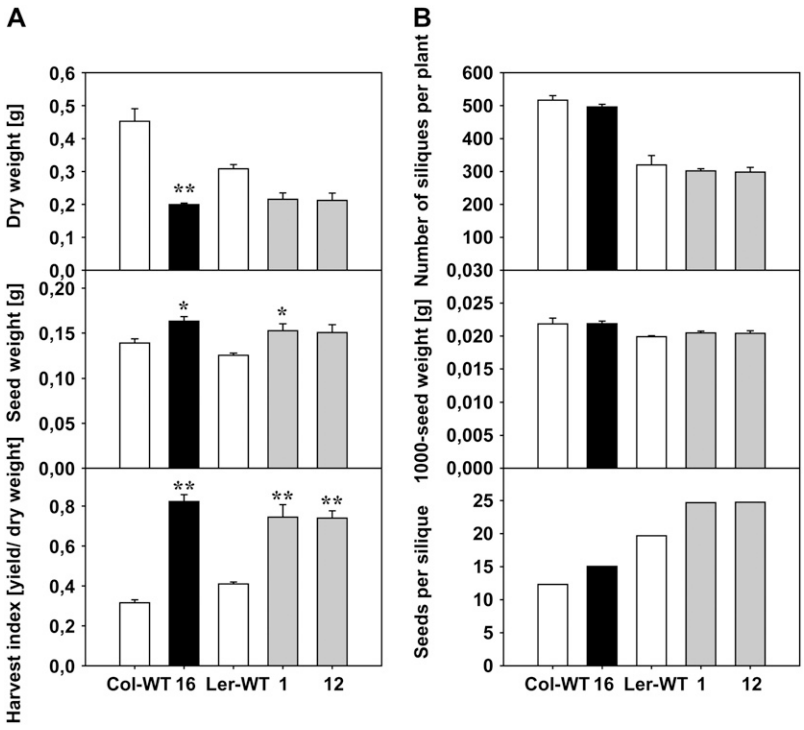

Figure 4. Harvest index and yield parameters in high-level MP17:GFP expressing Col-0 and L*er* lines. A, Total dry weight, seed yield, and calculated harvest index in lines Col-16, L*er*-1, and L*er*-12 in comparison to the corresponding ecotype controls. Plant were grown for 6 weeks under controlled SD conditions and subsequently maintained for additional 40 to 50 d under LD in a greenhouse until all plants were fully senescent and fruits started to open. Plants were kept dry for another 2 weeks before determination of total dry weight and seed mass. The harvest index was finally calculated as ratio between seed yield and total dry weight production. Data are presented as means ± SE of at least five individual plants per line. B, Number of siliques and the 1,000-seed weight were determined for individual plants of the indicated transgenic lines. Values indicate the mean ± SE of at least five individual plants per line. The average number of seeds per silique was finally calculated from the mean values of 1,000-seed weight, total seed yield, and number of siliques. Asterisks indicate statistical differences between transgenic lines and the respective wild type at *, $P < 0.05$; and **, $P < 0.01$ as determined by the Mann-Whitney *U*-test.

leaves raises the possibility of reduced MP17 accumulation in senescent leaves. Therefore, MP17:GFP protein levels were determined by means of western-blot analysis in the different leaf stages of Col-16. As demonstrated in Figure 5D, MP17:GFP protein levels continuously decreased upon leaf aging, suggesting either reduced transcriptional activity of the CaMV 35S promoter or proteolytic degradation of the MP17:GFP fusion protein with progressing leaf senescence. Analysis of MP17:GFP expression by northern-blot analysis indicated no major changes in transcript accumulation throughout all leaf stages (Fig. 5E), thereby excluding the possibility of reduced transgene expression. Consequently, we speculated that MP17:GFP showed reduced affinity to PD of older leaf stages and that nontargeted protein might be subjected to proteolytic degradation in these leaves. To test this hypothesis, plasmodesmal localization of MP17:GFP in epidermal cells was monitored throughout the different leaf stages of Col-16 by confocal laser scanner microscopy. As demonstrated in Figure 6, accumulation of MP17:GFP at PD continuously decreased with leaf age, suggesting the occurrence of significant structural and, potentially, also functional changes of PD in senescing leaves.

To assess alterations of PD function and symplastic transport capacity in different leaf stages upon MP17:GFP expression, we monitored the movement and phloem unloading of the membrane-impermanent fluorescent solute carboxyfluorescein (CF) in sink, source, and senescing leaves of Col-16 plants in comparison to the wild-type control. The tracer was loaded through cut petioles and allowed to distribute throughout the leaves, respectively. As shown in Figure 7, A to C, CF unloading from the phloem was clearly detectable in all three wild-type leaf stages. In contrast, symplastic trafficking out of the minor vein network in source leaves appeared to be clearly restricted in MP17:GFP expressing Col-16 plants, strongly indicating a MP17-mediated inhibition of symplastic continuity between cells of the vascular bundles and the surrounding mesophyll tissue (Fig. 7E). However, most likely due to the absence of MP17 from simple PD (see Fig. 1), massive movement of the fluorescent dye was observed in sink leaves of Col-16 (Fig. 7D). Importantly, a wild-type-like unloading pattern was also detectable in senescent leaves of the transgenic line (Fig. 7F), indicating that the reduced accumulation of MP17 protein at PD is sufficient to release the MP17-induced symplastic transport block detectable in source leaves.

DISCUSSION

Stable expression of MPs from different viruses in transgenic plants has previously been used to elucidate PD structure and functioning as well as the contribution of the symplastic pathway to assimilate transport and biomass partitioning. From these studies, the overall picture had emerged that association of MPs with branched PD significantly increases plasmodesmal conductivity in source leaves, however, with varying consequences for carbon metabolism, photoassimilate export, and growth performance. MP-induced effects appeared to be largely dependent on the selected MP, plant species, and cell types used for transgene

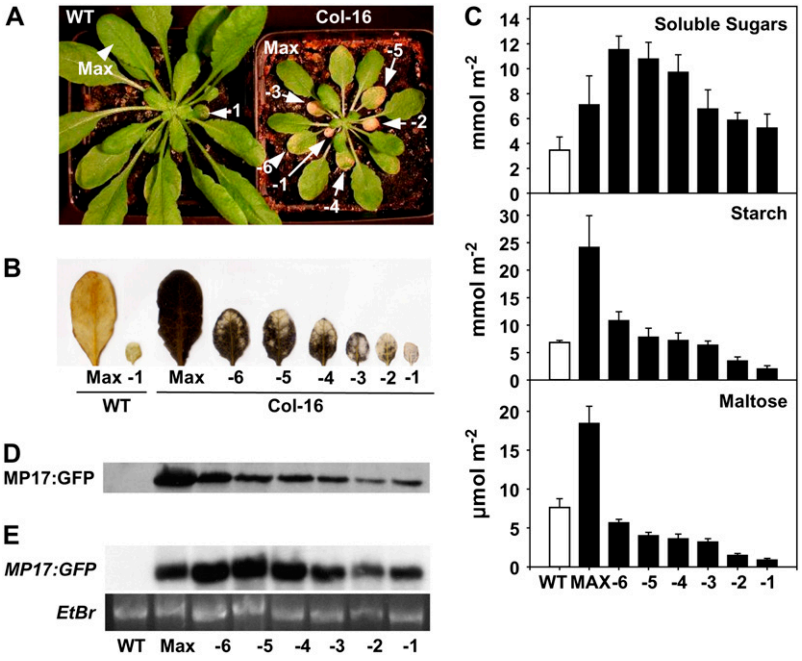

Figure 5. Release of the MP17-induced assimilate export block in senescing leaves of high-level MP17:GFP expressing Arabidopsis plants. A, Visible phenotype of MP17:GFP expressing line Col-16 grown for 66 d under SD conditions. Fully expanded source leaf (Max) and older leaf stages with progressing leaf senescence (-6 until -1 with the latter being defined as oldest leaf within the rosette) are indicated. B, Qualitative determination of starch accumulation in different senescing leaf stages of Col-16 and wild type after an extended dark period (16 h) by iodine (KI) staining. C, Carbohydrate levels in different senescing leaf stages of Col-16 in comparison to the fully expanded source leaves of the transgenic line (Max) and wild type. Samples for determination of soluble sugar, starch, and maltose were collected at the end of the dark period of 66-d-old plants. Values are given as mean ± SE of six (or five for maltose) individual plants, and soluble sugars represent the sum of Glc, Fru, and Suc. D, Western-blot analysis of MP17:GFP protein accumulation in different leaf stages of Col-16. Identical amounts of protein were separated by SDS-PAGE and immunodecorated using the polyclonal anti-MP17 antibody. E, Northern-blot analysis of *MP17:GFP* transcript accumulation. Each lane contains 25 μg of total RNA isolated from the indicated leaf stages of wild-type and Col-16 plants. Northern blots were hybridized with *MP17* cDNA (top section) and the ethydiumbromide stain (Etbr) of the RNA gel served as loading control (bottom section).

expression and were also shown to be developmentally regulated (Olesinski et al., 1996; Almon et al., 1997; Hofius et al., 2001; Shalitin et al., 2002; Mansilla et al., 2006). In this study, we constitutively expressed PLRV-MP17 fused to GFP in different Arabidopsis ecotypes to alter PD-mediated assimilate transport processes and observed significant changes of carbohydrate levels, vegetative biomass accumulation, and reproductive growth in a dosage-dependent manner. Low-level expression of MP17 increased leaf biomass production whereas high MP17 protein accumulation induced a severe growth penalty due to assimilate export deficiency of source leaves. However, reduced leaf biomass accumulation at high MP17 level was accompanied by enhanced seed production, giving rise to a strongly increased harvest index. This surprising effect seemed to be mediated by the release of the symplastic transport block in senescing leaves most likely due to decreasing MP17 accumulation at PD, which allowed the accumulated starch to be metabolized and the excess carbon pools to be allocated for the benefit of seed set and development.

MP17-GFP Localizes to Branched PD and Modifies Assimilate Allocation Most Likely by Perturbation of the Symplastic Connectivity of the Vasculature

Fluorescence and immunoelectron microscopy of transgenic Arabidopsis lines revealed localization of MP17:GFP to branched PD of various vascular and nonvascular cell types in source leaf and root tissue (Fig. 1, C–H), whereas simple PD of sink leaves were not targeted by MP17:GFP (Fig. 1, A and B). This localization pattern is very similar to the situation observed in MP17:GFP expressing tobacco plants (Hofius et al., 2001) and suggests an intrinsic and conserved ability of the MP from the solanaceous-adapted PLRV to target and modify the PD trafficking pathway, even in the nonhost Arabidopsis. This notion is supported by the finding that PD-localized MP17 was able to induce assimilate export deficiency and growth retardation in different Arabidopsis ecotypes (Figs. 2 and 3). Interestingly, the inhibition of Suc efflux from source leaves in high-level expressing Arabidopsis lines seemed to originate in the MP17-mediated interruption of the

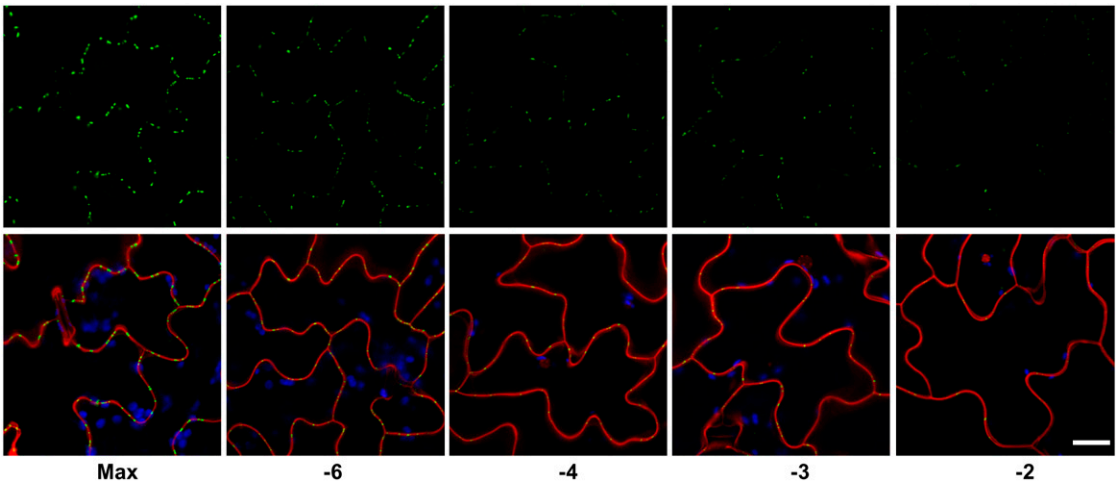

Figure 6. Reduced binding of MP17:GFP to PD during progression of leaf senescence. Epidermal cells of the indicated leaf stages from line Col-16 were scanned for MP17:GFP-derived fluorescence at PD by confocal laser scanning microscopy using identical settings for excitation and fluorescence detection. Images in the top section indicate GFP fluorescence displayed in green color. The bottom section shows superimposed images of green GFP fluorescence with chloroplasts in blue and propidiumiodine-stained cell wall and nuclei in red. Bar indicates 20 μm.

symplastic transport path between the mesophyll tissue and the vasculature as circumstantially suggested from the inability of CF to diffuse from the phloem into surrounding mesophyll cells in line Col-16 (Fig. 7). This observation appears to be consistent with previous electron microscopic studies of phenotypically altered leaves in MP17N-transgenic tobacco plants, showing distorted PD between phloem cells but not within the mesophyll tissue (Herbers et al., 1997). It also agrees with the apparent discrepancy that source leaves of both phenotypic and nonphenotypic MP17 transgenic tobacco lines showed increased plasmodesmal permeability in the mesophyll (Hofius et al., 2001). This suggested to us already before that the interaction of MP17 with PD of nonvascular tissue is probably not responsible for the assimilate export deficiency induced at high MP17 amounts in tobacco. Instead, we hypothesized indirect metabolic effects of MP17 causing sugar accumulation and growth retardation independent from altered SEL in the mesophyll tissue, or an expression level-dependent impact of MP17 specifically on PD function in the vascular bundle (Hofius et al., 2001). The latter scenario seems now to be supported by the results from MP17:GFP transgenic Arabidopsis lines in this study. Nevertheless, it remains to be elucidated in detail, for instance by means of cell-type-specific MP expression, which plasmodesmal connections in the vascular tissue are responsible for the observed changes, and whether the symplastic trafficking pathway is disrupted directly by the accumulation of large MP17 amounts or rather indirectly by MP-induced callose deposition at PD, as proposed for TSWV NS_M transgenic plants (Rinne et al., 2005). Interestingly, initial experiments seem to indicate that MP17-induced export deficiency is not accompanied by excessive callose accumulation and consistently, is not reversible by heat treatment as demonstrated for the NS_M expressing lines (data not shown).

Low-Level MP17-GFP Expression Leads to Higher Vegetative Biomass Production and Increased Suc Export Rates

In contrast to the apparent detrimental effect of high MP17 amounts on the Suc efflux pathway in source

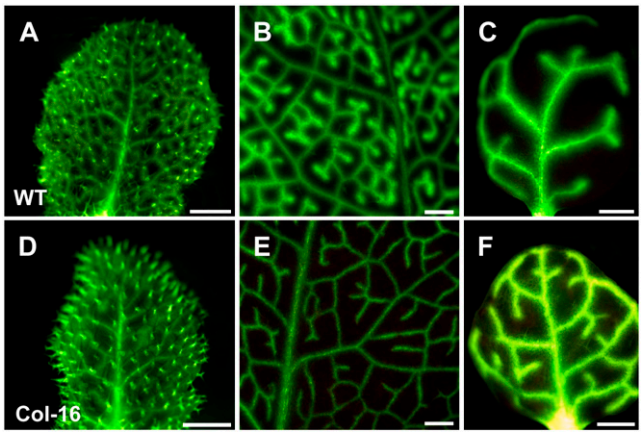

Figure 7. Symplastic unloading of CF from phloem in different leaf stages of Col-16 and wild type. A to C, Movement of CF from vascular bundles into the surrounding mesophyll tissue was detectable in sink (A), source (B), and senescent (C) leaves 10 min after inserting cut leaves with their petioles in the tracer solution. D to F, CF unloading in Col-16 could be observed in sink (D) and senescent (F) but not in source (E) leaves. Bar indicates 1 mm.

leaves leading to sugar accumulation and severe growth retardation, the increased leaf biomass production in low-level MP17 expressing Arabidopsis lines (Col-9 and C24-81; Fig. 2, G and H) seemed to be caused by improved capability for photoassimilate export and allocation. This assumption is supported by increased Suc efflux (Fig. 3, A and C) and concomitantly decreased levels of Suc and starch in source leaves (Table I), the latter has previously been observed in low-level expressing MP17N and MP17:GFP transgenic tobacco lines (Hofius et al., 2001). Similarly, increased Suc efflux rates caused by constitutive expression of CMV-MP and TMV-MP in melon (Shalitin et al., 2002) or by mesophyll-specific expression of TMV-MP in potato (Olesinski et al., 1996) were shown to be accompanied by decreased sugar levels in source leaves, indicating an improved symplastic transport capacity due to MP-mediated changes of plasmodesmal SEL. Although we did not probe plasmodesmal conductivity in source leaves of low-level expressing Arabidopsis lines, the intrinsic capability of MP17 to dilate mesophyll PD irrespective of the protein amount in tobacco plants (Hofius et al., 2001) suggests an increased plasmodesmal permeability in the mesophyll and/or in the phloem tissue as primary cause for increased Suc efflux, reduced carbohydrate accumulation, and improved vegetative growth performance in the Arabidopsis lines.

MP17:GFP-Mediated Modification of Suc Efflux Correlates with Accelerated or Delayed Flowering of Transgenic Arabidopsis Plants

Additional support for the assumption of increased nutrient flow to consuming sinks like the vegetative meristem in low-level MP17 expressing Col-0 and C24 seems to be provided by significantly accelerated floral transition under flower promoting, i.e. LD conditions (Fig. 2, J and K). It is well established that Suc has a stimulatory role on flowering induction at the shoot apical meristem in Arabidopsis and other plant species (Bernier et al., 1993; Corbesier et al., 1998; Roldan et al., 1999). Hence, changes in sink strength favoring assimilate supply, for instance by meristem-specific expression of yeast (*Saccharomyces cerevisiae*) cell wall invertase, caused accelerated flowering, whereas reduction in sink strength, mediated by transgenic expression of the invertase in the cytosol, delayed flowering (Heyer et al., 2004). In addition to this potentially direct effect of increased carbohydrate supply on flowering transition, increased assimilate allocation to the shoot apex might have indirectly stimulated phloem-mediated trafficking of signaling molecules such as *FLOWERING LOCUS* transcription factor, which has recently been shown to act as long-distance protein signal for flowering induction in Arabidopsis (Corbesier et al., 2007). The complementary effect of reduced assimilate export and supply to the shoot apical meristem (Fig. 2, J and L) seemed to be reflected by the strongly delayed transition to flowering in growth-retarded MP17 transgenic lines, although the severe reduction of biomass accumulation per se might equally well be the reason for the observed developmental delay. Nevertheless, the high-level MP17-induced assimilate export deficiency leading to severe growth penalty and delayed flowering was followed by improved reproductive growth, as manifested by partial compensation of the severe vegetative growth inhibition until maturity and, most remarkably, by significantly enhanced seed yield in both Col-0 and L*er* ecotypes (Figs. 2, M and O, and 4A). Determination of yield parameters demonstrated that the enhanced reproductive output was not the consequence of increased number of siliques or seed mass but rather due to an increased number of seeds per silique (Fig. 4B). Thus, we assume that improved resource allocation during seed set and development might have reduced the frequency of ovule abortion, a process that frequently occurs during reproduction, in particular in response to nutrient limitations and environmental stress (Sun et al., 2004, 2005).

High-Level Expression of MP17:GFP Improves Seed Yield and Harvest Index of Transgenic Arabidopsis Plants

Although high-level MP17 expressing transgenic lines were able to attenuate their dramatic vegetative growth retardation after floral induction, total biomass accumulation at harvest point reached only 60% to 70% of the respective wild type. Together with the concomitant increase in seed yield, a strongly improved harvest index could be achieved (Fig. 4A), which additionally demonstrated the MP17-mediated success in partitioning photoassimilate resources to the harvestable component. Changes in harvest index of cereal crops were formerly shown to be responsible for the large increases in global wheat (*Triticum aestivum*) and rice (*Oryza sativa*) yield during the green revolution (Hay, 1995; Sinclair, 1998). Beside new methods of cultivation, such progress was in particular made by introducing new varieties that showed a semidwarfed growth habit due to mutational changes in the biosynthesis or the signal transduction pathway of the GA growth hormone (Peng et al., 1999; Sasaki et al., 2002; Hedden, 2003). For instance, yield increase of superior rice varieties in response to incorporation of these dwarfing genes was the result of an improved harvest index from 0.3 to 0.5 (Hay, 1995). Remarkably, the increase in harvest index of MP17 transgenic Arabidopsis appeared in a similar range, as shown by the 1.8-fold enhancement in lines L*er*-1 and L*er*-12, or was even higher as demonstrated for Col-16 (2.8-fold; Fig. 4B). Thus, constitutive high-level MP17 expression might be an attractive strategy to control plant architecture and yield, potentially even in crop species distantly related to Arabidopsis. Similarly, the apparently ecotype-independent negative relationship between vegetative biomass accumulation and MP17 protein amount implies the potential for substantial increases in leaf biomass production by selecting for transgenic lines that accumulate MP17 only to low levels (Fig. 2).

PD Localization and Physiological Consequences of MP17:GFP Are under Developmental Control

The beneficial effect of MP17 on either vegetative or generative productivity at low and high expression levels, respectively, seems to be likewise mediated by alterations of the symplastic transport pathway via interaction with PD. However, the modes of action appear to be rather different. As discussed above, improved assimilate allocation at low-level MP17 amounts are directly caused by increased symplastic permeability and Suc efflux in mesophyll and/or vascular cells of source leaves. In contrast, accumulation of large amounts of MP17 at PD of vascular-associated cells initially interrupted symplastic permeability and the Suc transport pathway into the minor vein phloem, resulting in excess carbohydrate accumulation in source leaves. However, this deleterious impact of MP17 appeared reversible upon progression of plant age as indicated by the switch to increased Suc efflux after a prolonged growth period under LD conditions. Additional support for a senescence-associated alleviation of the MP17-induced disruption of symplastic transport and assimilate export was provided by reduced staining for starch accumulation (Fig. 5B), decreased amounts of PD-targeted MP17:GFP (Fig. 6), and unrestricted diffusion of CF from the minor vein network (Fig. 7) in older leaf stages compared to mature source leaves. Quantification of soluble sugars, starch, and maltose levels in these leaf stages further indicated that the accumulated starch was successively metabolized (Fig. 5C) and thus additional carbon resources made available for translocation into reproductive sinks after floral induction.

The observed decline in plasmodesmal localization and overall protein accumulation of MP17:GFP (Figs. 5D and 6) suggested the absence or reduced affinity of putative PD receptor proteins and subsequent proteolytic degradation of nontargeted MP17 in senescent leaves, strongly resembling the situation in sink leaves (Fig. 1; Vogel et al., 2007). In general, leaf senescence is regarded as a developmental process that is induced to recycle and mobilize nutrients for relocation to other plant organs such as reproducing seeds (Lim et al., 2006). Thus, it is tempting to assume that PD of senescent leaves need to provide a comparably high conductivity for symplastic transport of nutrients from mesophyll into the vascular tissue as proposed for the opposite direction in sink leaves (Imlau et al., 1999; Oparka et al., 1999). The nonselective and unrestricted transport capability observed for PD in sink leaves is considerably down-regulated during the importing-exporting transition for assimilates, and is paralleled by structural changes from simple to branched PD found in source tissue (Oparka et al., 1999). Although we did not analyze the ultrastructure of PD in senescent leaves in detail, our observation that PD of both sink and senescent leaves are apparently not targeted by MP17 indicates some structural and potentially also functional similarities. Thus, we speculate that the developmental and physiological transition of source leaves during leaf senescence is accompanied by changes in plasmodesmal architecture and conductivity, which lead to the formation of a distinct, yet unrecognized class of PD with at least some functional analogy to simple PD found in sink leaves.

CONCLUSION

Our work demonstrates the ability of PLRV-MP17 to alter PD functioning in terms of symplastic assimilate transport and resource allocation in Arabidopsis, and thus to improve leaf biomass and seed production in an inversely related and dosage-dependent manner. Furthermore, due to the penetrance of the MP17-mediated impact in different Arabidopsis ecotypes, the transgenic lines provide a novel and powerful tool for forward genetic approaches to identify cellular factors required for plasmodesmal targeting and trafficking as well as regulatory components involved in sink-source relations. Finally, our data indicate structural and potentially functional changes of PD during leaf senescence that might be related to the requirement for efficient and unrestricted relocation of recycled and mobilized resources for reproductive success.

MATERIALS AND METHODS

Plant Material and Growth Conditions

Arabidopsis (*Arabidopsis thaliana*) ecotypes Col-0, C24, and L*er* were maintained in Klasman substrate number 1 compost (Klasmann-Deilmann GmbH) under controlled SD condition in a growth chamber (8 h day/16 h night regime with 20°C/18°C, 60% humidity, 120 μM m^{-2} s^{-1} light). For induction of reproductive growth, plants were transferred to LD conditions in a temperature-controlled greenhouse (20°C day/18°C night) with 16 h supplementary light (100 μM m^{-2} s^{-1}) and 8 h darkness. For selection of transgenic plants, seeds were sterilized and sown onto Murashige Skoog medium (Sigma) supplemented with Gamborg's vitamin solution (1:1,000) and 50 μg/mL kanamycin. Plants were given cold treatment for 2 d to synchronize germination before incubation under a 16-h-light/8-h-dark photoperiod (150 μM m^{-2} s^{-1} light, 21°C) at 50% relative humidity.

Plant Transformation

Transformation of different Arabidopsis ecotypes with the previously described binary construct p35S-1, harboring an in-frame gene fusion of PLRV-*MP17* and *GFP* under control of the CaMV 35S promoter (Hofius et al., 2001), was performed with the *Agrobacterium tumefaciens* strain CV58C1 (containing the pGV2260 helper plasmid) according to Bechtold and Pelletier (1998) or Clough and Bent (1998).

Western-Blot Analysis and MP17 Protein Quantification

Samples of Arabidopsis leaves corresponding to 0.81 cm^2 were homogenized in 2× SDS sample buffer containing 50 mM Tris-HCl, 5% (v/v) β-mercaptoethanol, 10% (v/v) Glycerin, 2% (w/v) SDS, pH 6.8. After heat denaturation for 10 min, the debris was centrifuged and equal amounts of supernatants were separated on 12.5% (v/v) SDS-polyacrylamid gels. Subsequent protein transfer, incubation with rabbit anti-PLRV-MP17 antibody (1:5,000), and development of immunoblots were followed exactly the procedures described in Hofius et al. (2001). Signals were quantified by means of an imaging analyzer (Molecular Imager System, Bio-Rad) and normalization of western blots was performed by additional probing with an anti-Transketolase antiserum (1:5,000) according to Hofius et al. (2001).

Northern-Blot Analysis

Extraction of total RNA from leaf material and northern-blot analysis was performed as described by Chen et al. (2003). *MP17:GFP* specific transcripts were detected using a random-primed [^{32}P]labeled cDNA fragment.

Carbohydrate Determination

Soluble sugars and starch levels were determined in leaf samples extracted with either 80% (v/v) ethanol/20 mM HEPES, pH 7.5 (Table I), or 80% (v/v) ethanol/10 mM EDTA, pH 7.5 (Fig. 4D) as described (Sonnewald, 1992). Maltose was measured from the same extracts with HPLC using the conditions exactly as described (Börnke et al., 2001). Starch accumulation in leaves was visualized by iodine staining (1% [w/v] I_2, 2% [w/v] KI) after an extended dark period (16 h), and chlorophyll was removed by incubation in 80% (v/v) ethanol/10 mM EDTA at 55°C.

Determination of Biomass Production, Flowering Time, and Yield Parameters

To assay vegetative and reproductive growth, seeds were sown in soil and kept under controlled SD conditions (see above) for 10 d until seedlings were transferred individually to new pots. Vegetative biomass accumulation corresponding to the fresh weight of the entire leaf rosette without the root system was determined after an additional period of 32 d under SD (see above). To measure reproductive growth, an additional set of plants grown under the same conditions for 6 weeks was transferred to LD conditions (see above) and flowering induction of the transgenic lines was recorded by counting the days from the date of transfer until the appearance of the first open flower. Plant lines were subsequently maintained for a period of 40 to 50 d under temperature-controlled greenhouse conditions (see above) until all plants were completely senescent and fruits on the main inflorescence started to open. After plants were kept dry for additional 2 weeks, total dry weight, number of siliques, total seed weight, and 1,000-seed weight was determined for each individual plant and the harvest index (ratio between seed weight and total biomass) and the average number of seeds per silique was calculated.

Determination of Suc Efflux from Source Leaves

Collection of phloem exudates for Suc efflux analysis was performed at two different time points, with plants grown for 6 weeks under SD condition (vegetative stage) and additional 3 weeks under LD condition (reproductive stage). At the latter growth stage, all plants had developed stems and flowers and initial signs of leaf senescence could be detected. Two mature source leaves per plant were detached by cutting petioles close to the stem. Excised petioles were immediately placed in a 1.5 mL test tube containing 200 μL of 5 mM EDTA, and exudates were collected for 6 h under conditions of 150 μM m^{-2} s^{-1} supplementary light and water-saturated atmosphere (Corbesier et al., 1998). Aliquots were sampled from the exudates after 1, 2, 4, and 6 h, and Suc content was determined as described above.

Confocal Laser Scanning and Immunoelectron Microscopy

Detection of MP17:GFP fusion protein-derived fluorescence signals in manual sections of leaf and root tissue from different transgenic lines was performed by confocal laser scanning microscopy according to Hofius et al. (2001). For comparison of MP17:GFP fluorescence signals in different leaf stages, leaves were manually cut and epidermal cells scanned using a Leica TCS SP2 laser scanning microscope (Leica Microsystems). Cell walls were stained with a saturated solution of propidiumiodide (5 mg/mL) for 5 to 10 min followed by up to six washing steps with water. Using a 488 nm 20 mW argon laser, GFP emission was detected from 497 to 526 nm, chlorophyll from 682 to 730 nm, and propidiumiodine from 598 to 650 nm. The different fluorescence signals were superimposed and equally processed using the Leica Confocal Software 2.5.

Fixation, embedding, and immunogold labeling of leaf and root sections with anti-MP17 as primary antibody followed exactly the protocol described in Hofius et al. (2001). Identical treatments of sections from wild-type plants revealed no labeling of PD structures, confirming the specificity of the antibody.

CF Movement

To monitor symplastic unloading of CF from vascular bundles, different leaf stages (sink, source, and senescent leaves) of line Col-16 and wild type were cut and inserted with their petioles in capillaries containing 2 mM carboxyfluoresceindiacetate (prepared by diluting a stock solution of 13 mM in acetone with water/5 mM KOH; Molecular Probes Inc.). CF-specific fluorescence was detected 10 min after loading using a Leica MZ16F stereomacroscope, a Leica DFC480 fluorescence camera, and Leica IM500 Image Manager software.

Statistical Analysis

Differences between transgenic lines and the corresponding wild type were compared using the nonparametric Mann-Whitney *U*-test, since most data were found to lack the assumption of normal distribution and homogeneity of variance. All statistical analyses were performed with Analyze-it v2.03 beta.

ACKNOWLEDGMENTS

We wish to thank Bernhard Claus (Institut für Pflanzengenetik und Kulturpflanzenforschung Gatersleben) for skillful help with confocal laser scanning microscopy and Marc Strickert (Institut für Pflanzengenetik und Kulturpflanzenforschung Gatersleben) for valuable advice on the statistical analysis. We also like to thank Norbert Sauer (Friedrich-Alexander-Universität Erlangen-Nürnberg, Germany) for providing the confocal laser scanning microscope of his department.

Received May 25, 2007; accepted September 4, 2007; published September 7, 2007.

LITERATURE CITED

Almon E, Horowitz M, Wang HL, Lucas WJ, Zamski E, Wolf S (1997) Phloem-specific expression of the tobacco mosaic virus movement protein alters carbon metabolism and partitioning in transgenic potato plants. Plant Physiol **115:** 1599–1607

Balachandran S, Hull RJ, Vaadia Y, Wolf S, Lucas WJ (1995) Alteration in carbon partitioning induced by the movement protein of tobacco mosaic virus originates in the mesophyll and is independent of change in the plasmodesmal size exclusion limit. Plant Cell Environ **18:** 1301–1310

Baluska F, Cvrckova F, Kendrick-Jones J, Volkmann D (2001) Sink plasmodesmata as gateways for phloem unloading: myosin VIII and calreticulin as molecular determinants of sink strength? Plant Physiol **126:** 39–46

Bechtold N, Pelletier G (1998) *In planta* Agrobacterium-mediated transformation of adult *Arabidopsis thaliana* plants by vacuum infiltration. Methods Mol Biol **82:** 259–266

Bernier G, Havelange A, Houssa C, Petitjean A, Lejeune P (1993) Physiological signals that induce flowering. Plant Cell **5:** 1147–1155

Börnke F, Hajirezaei M, Sonnewald U (2001) Cloning and characterization of the gene cluster for palatinose metabolism from the phytopathogenic bacterium Erwinia rhapontici. J Bacteriol **183:** 2425–2430

Chen S, Hofius D, Sonnewald U, Bornke F (2003) Temporal and spatial control of gene silencing in transgenic plants by inducible expression of double-stranded RNA. Plant J **36:** 731–740

Chia T, Thorneycroft D, Chapple A, Messerli G, Chen J, Zeeman SC, Smith SM, Smith AM (2004) A cytosolic glucosyltransferase is required for conversion of starch to sucrose in Arabidopsis leaves at night. Plant J **37:** 853–863

Clough SJ, Bent AF (1998) Floral dip: a simplified method for Agrobacterium-mediated transformation of Arabidopsis thaliana. Plant J **16:** 735–743

Corbesier L, Lejeune P, Bernier G (1998) The role of carbohydrates in the induction of flowering in Arabidopsis thaliana: comparison between the wild type and a starchless mutant. Planta **206:** 131–137

Corbesier L, Vincent C, Jang S, Fornara F, Fan Q, Searle I, Giakountis A, Farrona S, Gissot L, Turnbull C, et al (2007) FT protein movement contributes to long-distance signaling in floral induction of Arabidopsis. Science **316:** 1030–1033

Crawford KM, Zambryski PC (2001) Non-targeted and targeted protein movement through plasmodesmata in leaves in different developmental and physiological states. Plant Physiol **125:** 1802–1812

Ding B, Haudenshield JS, Hull RJ, Wolf S, Beachy RN, Lucas WJ (1992) Secondary plasmodesmata are specific sites of localization of the Tobacco Mosaic Virus movement protein in transgenic tobacco plants. Plant Cell **4:** 915–928

Haupt S, Duncan GH, Holzberg S, Oparka KJ (2001) Evidence for symplastic phloem unloading in sink leaves of barley. Plant Physiol **125:** 209–218

Hay RKM (1995) Harvest index—a review of its use in plant-breeding bnd crop physiology. Ann Appl Biol **126:** 197–216

Hedden P (2003) The genes of the green revolution. Trends Genet **19:** 5–9

Herbers K, Tacke E, Hazirezaei M, Krause KP, Melzer M, Rhode W, Sonnewald U (1997) Expression of a luteoviral movement protein in transgenic plants leads to carbohydrate accumulation and reduced photosynthetic capacity in source leaves. Plant J **12:** 1045–1056

Heyer AG, Raap M, Schroeer B, Marty B, Willmitzer L (2004) Cell wall invertase expression at the apical meristem alters floral, architectural, and reproductive traits in *Arabidopsis thaliana*. Plant J **39:** 161–169

Hofius D, Herbers K, Melzer M, Omid A, Tacke E, Wolf S, Sonnewald U (2001) Evidence for expression level-dependent modulation of carbohydrate status and viral resistance by the potato leafroll virus movement protein in transgenic tobacco plants. Plant J **28:** 529–543

Hoth S, Schneidereit A, Lauterbach C, Scholz-Starke J, Sauer N (2005) Nematode infection triggers the de novo formation of unloading phloem that allows macromolecular trafficking of green fluorescent protein into syncytia. Plant Physiol **138:** 383–392

Imlau A, Truernit E, Sauer N (1999) Cell-to-cell and long-distance trafficking of the green fluorescent protein in the phloem and symplastic unloading of the protein into sink tissues. Plant Cell **11:** 309–322

Itaya A, Woo YM, Masuta C, Bao Y, Nelson RS, Ding B (1998) Developmental regulation of intercellular protein trafficking through plasmodesmata in tobacco leaf epidermis. Plant Physiol **118:** 373–385

Kim I, Zambryski PC (2005) Cell-to-cell communication via plasmodesmata during *Arabidopsis* embryogenesis. Curr Opin Plant Biol **8:** 593–599

Lazarowitz SG, Beachy RN (1999) Viral movement proteins as robes for intracellular and intercellular trafficking in plants. Plant Cell **11:** 535–548

Liarzi O, Epel BL (2005) Development of a quantitative tool for measuring changes in the coefficient of conductivity of plasmodesmata induced by developmental, biotic, and abiotic signals. Protoplasma **225:** 67–76

Lim PO, Kim HJ, Nam HG (2006) Leaf senescence. Annu Rev Plant Biol **58:** 115–136

Lu Y, Sharkey TD (2006) The importance of maltose in transitory starch breakdown. Plant Cell Environ **29:** 353–366

Lucas WJ (2006) Plant viral movement proteins: agents for cell-to-cell trafficking of viral genomes. Virology **344:** 169–184

Lucas WJ, Balachandran S, Park J, Wolf S (1996) Plasmodesmal companion cell-mesophyll communication in the control over carbon metabolism and phloem transport: insights gained from viral movement proteins. J Exp Bot **47:** 1119–1128

Lucas WJ, Lee JY (2004) Plasmodesmata as a supracellular control network in plants. Nature **5:** 712–726

Lucas WJ, Olesinski A, Hull RJ, Haudenshield JS, Deom CM, Beachy RN, Wolf S (1993) Influence of the Tobacco Mosaic Virus 30 kDa movement protein on carbon metabolism and photosynthate partitioning in transgenic tobacco plants. Planta **190:** 88–96

Lucas WJ, Wolf S (1999) Connections between virus movement, macromolecular signaling and assimilate allocation. Curr Opin Plant Biol **2:** 192–197

Mansilla C, Aguilar I, Martinez-Herrera D, Sanchez F, Ponz F (2006) Physiological effects of constitutive expression of Oilseed Rape Mosaic Tobamovirus (ORMV) movement protein in *Arabidopsis thaliana*. Transgenic Res **15:** 761–770

Niittyla T, Messerli G, Trevisan M, Chen J, Smith AM, Zeeman SC (2004) A previously unknown maltose transporter essential for starch degradation in leaves. Science **303:** 87–89

Olesinski AA, Almon E, Navot N, Perl A, Galun E, Lucas WJ, Wolf S (1996) Tissue-specific expression of the Tobacco Mosaic Virus movement protein in transgenic potato plants alters plasmodesmal function and carbohydrate partitioning. Plant Physiol **111:** 541–550

Olesinski AA, Lucas WJ, Galun E, Wolf S (1995) Pleiotropic effects of Tobacco Mosaic Virus movement protein on carbon metabolism in transgenic tobacco plants. Planta **197:** 118–126

Oparka KJ (2004) Getting the message across: how do plant cells exchange macromolecular complexes? Trends Plant Sci **9:** 33–41

Oparka KJ, Roberts AG, Boevenik P, Santa Cruz S, Roberts I, Pradel KS, Imlau A, Kotlizky G, Sauer N, Epel B (1999) Simple, but not branched, plasmodesmata allow the nonspecific trafficking of proteins in developing tobacco leaves. Cell **97:** 743–754

Peng J, Richards DE, Hartley NM, Murphy GP, Devos KM, Flintham JE, Beales J, Fish LJ, Worland AJ, Pelica F, et al (1999) ''Green revolution'' genes encode mutant gibberellin response modulators. Nature **400:** 256–261

Rinne PLH, van den Boogaard R, Mensink MGJ, Kopperud C, Kormelink R, Goldbach R, van der Schoot C (2005) Tobacco plants respond to the constitutive expression of the tospovirus movement protein NS_M with a heat-reversible sealing of plasmodesmata that impairs development. Plant J **43:** 688–707

Roberts AG, Oparka KJ (2003) Plasmodesmata and the control of symplastic transport. Plant Cell Environ **26:** 103–124

Roberts IM, Boevink P, Roberts AG, Sauer N, Oparka KJ (2001) Dynamic changes in the frequency and architecture of plasmodesmata during the sink-source transition in tobacco leaves. Protoplasma **218:** 31–44

Roldan M, Gomez-Mena C, Ruiz-Garcia L, Salinas J, Martinez-Zapater JM (1999) Sucrose availability on the aerial part of the plant promotes morphogenesis and flowering of Arabidopsis in the dark. Plant J **20:** 581–590

Ruiz-Medrano R, Xoconostle-Cazares B, Kragler F (2004) The plasmodesmatal transport pathway for homeotic proteins, silencing signals and viruses. Curr Opin Plant Biol **7:** 641–650

Sasaki A, Ashikari M, Ueguchi-Tanaka M, Itoh H, Nishimura A, Swapan D, Ishiyama K, Saito T, Kobayashi M, Khush GS, et al (2002) Green revolution: a mutant gibberellin-synthesis gene in rice. Nature **416:** 701–702

Shalitin D, Wang Y, Omid A, Gal-On A, Wolf S (2002) Cucumber mosaic virus movement protein affects sugar metabolism and transport in tobacco and melon plants. Plant Cell Environ **25:** 989–997

Sinclair TR (1998) Historical changes in harvest index and crop nitrogen accumulation. Crop Sci **38:** 638–643

Sonnewald U (1992) Expression of E. coli inorganic pyrophosphatase in transgenic plants alters photoassimilate partitioning. Plant J **2:** 571–581

Stitt M (1996) Plasmodesmata play an essential role in sucrose export from leaves: a step toward an integration of metabolic biochemistry and cell biology. Plant Cell **8:** 565–571

Sun K, Cui Y, Hauser BA (2005) Environmental stress alters genes expression and induces ovule abortion: reactive oxygen species appear as ovules commit to abort. Planta **222:** 632–642

Sun K, Hunt K, Hauser BA (2004) Ovule abortion in Arabidopsis triggered by stress. Plant Physiol **135:** 2358–2367

Viola R, Roberts AG, Haupt S, Gazzani S, Hancock RD, Marmiroli N, Machray GC, Oparka KJ (2001) Tuberization in potato involves a switch from apoplastic to symplastic phloem unloading. Plant Cell **13:** 385–398

Vogel F, Hofius D, Sonnewald U (July 11, 2007) Intracellular trafficking of potato leafroll virus movement protein in transgenic Arabidopsis. Traffic **8:** 1205–1214

Waigmann E, Lucas WJ, Citovsky V, Zambryski P (1994) Direct functional assay for tobacco mosaic virus cell-to-cell movement protein and identification of a domain involved in increasing plasmodesmal permeability. Proc Natl Acad Sci USA **91:** 1433–1437

Wolf S, Deom CM, Beachy R, Lucas WJ (1989) Movement protein of tobacco mosaic virus modifies plasmodesmatal size exclusion limit. Science **246:** 377–379

Wolf S, Deom CM, Beachy R, Lucas WJ (1991) Plasmodesmatal function is probed using transgenic tobacco plants that express a virus movement protein. Plant Cell **3:** 593–604

Zambryski P (2004) Cell-to-cell transport of proteins and fluorescent tracers via plasmodesmata during plant development. J Cell Biol **164:** 165–168